

## Structural investigation of caffeine monolayers on Au(111)

Malte G. H. Schulte <sup>1,2</sup>, Andreas Jeindl <sup>3</sup>, Ismail Baltaci <sup>1,2</sup>, Peter Roesch <sup>1,2</sup>, Marie Schmitz <sup>1,2</sup>, Ulf Berges,<sup>1,2</sup>  
Oliver T. Hofmann,<sup>3</sup> and Carsten Westphal<sup>1,2</sup>

<sup>1</sup>*Experimentelle Physik I, Technische Universität Dortmund, Otto-Hahn-Strasse 4, D-44221, Dortmund, Germany*

<sup>2</sup>*DELTA, Technische Universität Dortmund, Maria-Goeppert-Mayer-Strasse 2, D-44221, Dortmund, Germany*

<sup>3</sup>*Institut für Festkörperphysik, NAWI Graz, Technische Universität Graz, Petersgasse 16, A-8010 Graz, Austria*



(Received 11 October 2019; revised manuscript received 26 May 2020; accepted 28 May 2020; published 11 June 2020)

The asymmetric and achiral character of caffeine ( $C_8H_{10}N_4O_2$ ) leads to two on-surface chiralities which has an impact on its on-surface formation. An analysis of its on-surface behavior reveals new insights of its crystallite growth. In this study the structural formation of caffeine monolayers on a Au(111) surface was analyzed by scanning tunneling microscopy (STM), low energy electron diffraction (LEED), x-ray photoelectron spectroscopy (XPS), and density functional theory (DFT) calculations. The monolayers were prepared by molecular beam epitaxy (MBE) and analyzed at room temperature. Caffeine molecules self-assemble in a quasihexagonal phase on Au(111) similar to the high-temperature  $\alpha$  phase. Two mirrored hexagonal domains are present with respect to the surface. Within the XPS measurements, no strong surface interaction was found. Therefore, a theoretical analysis of a hypothetical free-standing caffeine monolayer structure was performed by *ab initio* simulations. We found that a caffeine monolayer with three molecules per unit cell is preferable to one with just a single molecule, as could be expected from the LEED pattern.

DOI: [10.1103/PhysRevB.101.245414](https://doi.org/10.1103/PhysRevB.101.245414)

### I. INTRODUCTION

Structurally, caffeine bulk crystals show a polymorphic behavior with a stable  $\beta$  phase and a metastable high-temperature  $\alpha$  phase [1]. In 2005 and 2007, the structures of the  $\alpha$  and  $\beta$  phase were determined by Derollez *et al.* [2] and Lehmann *et al.* [3], respectively.

The fabrication of thin layers of caffeine gathered interest in recent years and structural investigations of caffeine crystal growth in thin films on various substrates were performed [4–6]. Especially the study of the growth process for defined fabrication of organic thin films is of interest and Röthel *et al.* found preferable orientations of caffeine crystals on ionic substrates like mica, NaCl, and KCl [7].

As the caffeine molecule is a xanthine derivative with the molecular structure shown in Fig. 1, the asymmetric and achiral character of it leads to two on-surface chiralities. This prochiral character could have an impact on its monolayer formation [8,9]. A similar behavior was found for the related xanthine derivative theophylline on Au(111) [10]. Therefore, an analysis of the monolayer of the asymmetric caffeine molecule reveals insights into the molecule-substrate interaction and its on-surface assembly which could lead to preferable orientations with respect to the substrate. To study these interactions and the influence of the on-surface chirality of caffeine in a combined theoretical and experimental approach, we used a Au(111) surface as a simple and accessible model system.

Hence, we report on the monolayer formation of caffeine on Au(111) characterized by scanning tunneling microscopy (STM), low-energy electron diffraction (LEED), x-ray

photoelectron spectroscopy (XPS), and density functional theory (DFT) calculations.

### II. EXPERIMENTAL SETUP

#### A. Sample preparation

Commercially available anhydrous caffeine powder from Sigma-Aldrich, with purity > 99%, was used in our investigation. In order to obtain caffeine monolayers, the molecules were evaporated by molecular beam epitaxy (MBE) from a Knudsen effusion cell [11] in an UHV chamber. The base pressure was below  $5 \times 10^{-10}$  mbar. The Au(111) substrate was obtained from MaTecK with a purity of 99.999%. A clean, reconstructed surface was prepared by repeated cycles of Ar<sup>+</sup> sputtering with a kinetic energy of  $E_{\text{kin}} = 800$  eV and at an incidence angle of  $\Theta = 45^\circ$ , followed by annealing at  $T \sim 700^\circ\text{C}$ .

The caffeine film thickness determination was performed by a quartz crystal microbalance (QCM) and a TM14 thickness monitor by PREVAC, assuming the density of the high-temperature  $\alpha$  phase ( $\rho = 1.45$  g cm<sup>-3</sup>) [2]. The monolayer height was approximated to one half of the height of the  $\alpha$ -phase unit cell with  $h_{\text{mono}} = \frac{\epsilon}{2} = 3.45$  Å, which consists of two different layers of caffeine molecules [2].

At standard conditions, caffeine powder sublimates at 178 °C [12]. At a base pressure of  $5 \times 10^{-10}$  mbar and a sublimation temperature of 85 °C, we measured rates of  $\sim 0.005$  Å s<sup>-2</sup> caffeine deposition with the QCM. In order to decrease the deposition time, an evaporation temperature of 100 °C was used while preparing the sample. The sublimation process was checked by analyzing the residual gas with a

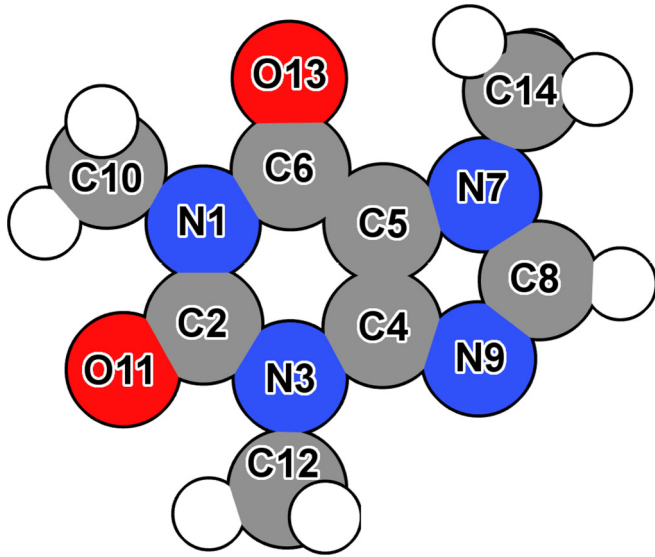


FIG. 1. Molecular structure of caffeine ( $C_8H_{10}N_4O_2$ ) and assignment of numbers to atoms within the molecule.

quadrupole mass spectrometer. The characteristic caffeine cracking pattern, including the main peak at 194 u indicating intact caffeine molecules, was observed [13].

Furthermore, the XPS measurements of the adsorbed monolayer reveal results similar to the XP spectra of gas-phase caffeine [14], indicating intact caffeine molecules on the surface. Also, the XP spectra of the Au 4*f* signal remain intact without any spectroscopic hint of a chemical bond between Au and caffeine as shown in the Supplemental Material [15].

Before deposition, the caffeine powder was carefully degassed at  $\sim 70^\circ\text{C}$ . Deposition of one monolayer caffeine was achieved by applying a Knudsen cell temperature of  $T \sim 100^\circ\text{C}$  for  $\sim 120$  s with a deposition rate of  $\sim 0.03 \text{ \AA s}^{-2}$ . The results of the film thickness determined by QCM were confirmed by XPS. After deposition, well-ordered caffeine monolayer films were achieved by heating the substrate to  $\sim 80^\circ\text{C}$  for  $\sim 10$  min. LEED was used to verify the surface reconstruction and to check the quality of the monolayer.

### B. STM measurements

All STM measurements were performed at room temperature with an Omicron STM using an electrochemical etched tungsten tip, which was prepared *in situ*. Voltage and current set points were adapted for each measurement to obtain the best result. Post processing, lattice constant determination, and data visualization of the STM measurements were carried out by the software package Gwyddion [16]. The lattice constants were determined from the STM measurements using 2D-fast Fourier transform (FFT) and autocorrelation function (ACF).

### C. XPS measurements

XPS measurements were performed at beamline 11 at the synchrotron radiation facility DELTA, TU Dortmund,

Germany [17]. For these measurements, the *in situ* preparation was repeated at a base pressure of  $5 \times 10^{-11}$  mbar.

For a quantitative analysis, a peak fitting procedure was carried out for all XP spectra in order to precisely determine peak intensities and different chemical bonding environments. A convolution of Doniach-Sunjić and Gauss functions was applied to all XP spectra [18]. With this line shape and a Tougaard background, the asymmetric shape of transition metals and metalized elements can be described [19]. Also, for the adsorbed molecular spectra, an asymmetric line shape is common [20]. The UNIFIT 2017 software package [21] was used since it offers a variety of in-depth XPS analysis procedures, such as applying fit functions and a Tougaard background as previously mentioned.

### D. Density functional theory calculations

DFT calculations were performed using the FHI-aims package [22] with a “tight” basis set (as shipped with the FHI-aims package) and the exchange-correlation functional PBE [23]. Long-range dispersion was included via the  $\text{TS}^{\text{surf}}$  correction [24]. For all DFT calculations, the following self-consistency thresholds were used:  $1 \times 10^{-6}$  eV for the total energy,  $1 \times 10^{-6}$  electrons for the total density, and  $1 \times 10^{-3}$  eV for the sum of eigenvalues. The interaction between individual molecules was calculated using open boundary conditions. To calculate the caffeine/gold interface system we employed the repeated slab approach with a  $7 \times 7 \times 1$  Monkhorst-Pack [25] *k*-point grid, a cell height of 80  $\text{\AA}$ , and dipole correction [26] to electrostatically decouple vertical replicas of the system. As a substrate we used a slab consisting of four layers of gold with a lattice constant of 4.175  $\text{\AA}$ . For the occupation of the bands we used Gaussian broadening with a width of 0.1 eV. The geometry optimization was performed with fixed substrate and relaxing the molecules until the remaining forces fell below force threshold of  $0.05 \text{ eV \AA}^{-1}$ .

For the diffraction simulation the geometry-optimized on-surface structure of caffeine was used, but without the substrate, i.e., as a free-standing monolayer. To simulate the diffraction pattern, kinematic diffraction theory was used. Specifically, the location and intensity of the peaks was calculated using the square of the structure factors  $n_{\vec{G}} = \sum_{\text{atoms}} f_{\text{atom}}(\vec{G}) \times \exp(-i\vec{G}\vec{r}_{\text{atom}})$  where  $\vec{G}$  and  $\vec{r}_{\text{atom}}$  are the reciprocal lattice vectors of the crystal and the location of atoms in the unit cell, respectively. The atomic form factors were calculated with  $f_{\text{atom}}(\vec{G}) = \sum_{i=1}^n a_i \exp[-b_i(\frac{\vec{G}}{4\pi})^2]$  with  $a_i$  and  $b_i$  taken from [27].

## III. RESULTS AND DISCUSSION

### A. Dense monolayer formation

Dense caffeine monolayers were prepared by substrate heating at  $\sim 80^\circ\text{C}$  for  $\sim 10$  min after molecular deposition of nominally  $\sim 1.3$  ML. Using this method, we found a caffeine molecule assembly on Au(111), as shown in an overview image in Fig. 2(a). At this coverage, the STM images show a homogeneous, ordered molecular film with some caffeine islands on top. A closer look at the phase is shown in Fig. 2(b),

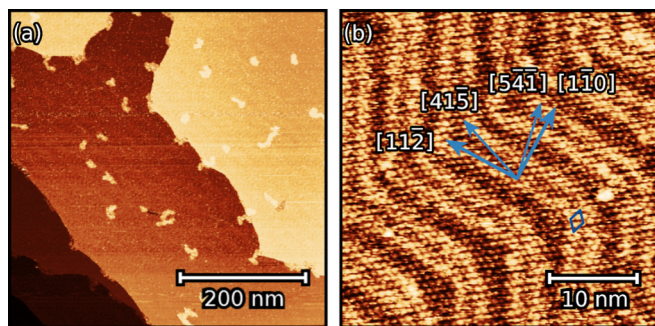


FIG. 2. STM images of caffeine adsorbed on Au(111). (a) After heating the substrate at  $80^\circ\text{C}$  for 10 min the caffeine film of  $\sim 1.3$  ML coverage is found homogeneous with some islands on top ( $500 \times 500$  nm, 10 pA,  $-2.0$  V). (b) Close-up view of the surface with hexagonal caffeine monolayer formation on Au(111). An angle of  $10 \pm 3^\circ$  was observed between the substrate  $[1\bar{1}0]$  direction and the caffeine  $[5\bar{4}1]$  direction. ( $36 \times 36$  nm, 17 pA,  $-1.0$  V).

and will be discussed in more detail later. At lower coverages, it is more likely that the STM tip drags molecules across the surface, which limits the resolution. As a consequence, we were not able to find densely packed caffeine molecules at lower coverages at room temperature with the STM.

Figure 3 shows STM images of a caffeine monolayer on Au(111). The averaged nearest neighbor distance of caffeine molecules in the STM images is  $8.7(9)$  Å with an angle of  $60 \pm 3^\circ$  between two nearest neighbors. Beneath the adsorbed

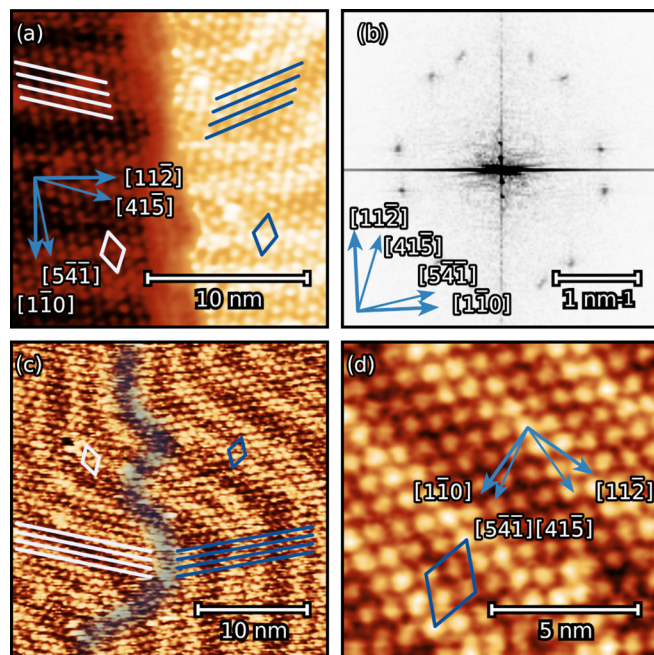


FIG. 3. (a) STM image of a caffeine monolayer on Au(111) with two mirrored film domains separated by a substrate step edge ( $19 \times 19$  nm, 16 pA,  $-1.0$  V). (b) Fast Fourier transform corresponding to (a) showing 12 spots. (c) Domain border of a dense caffeine monolayer on the same substrate terrace ( $28 \times 28$  nm, 17 pA,  $-1.0$  V). (d) STM image of a caffeine monolayer on Au(111) ( $11 \times 11$  nm, 15 pA,  $-1.0$  V).

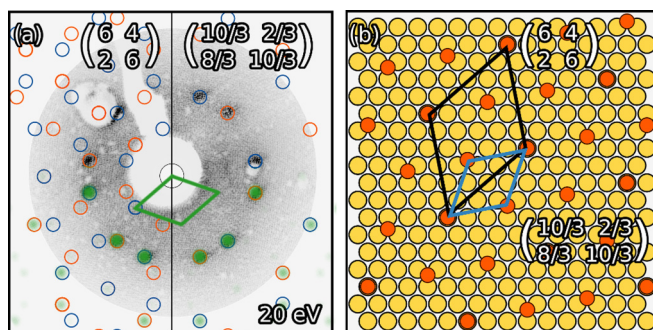


FIG. 4. (a) LEED pattern of the caffeine monolayer formation on Au(111) recorded at an electron energy of  $E_{\text{kin}} = 20$  eV. On top of the LEED image the LEEDpat simulation of a  $\begin{pmatrix} 6 & 4 \\ 2 & 6 \end{pmatrix}$  or  $2\sqrt{7}$  and a  $\begin{pmatrix} 10/3 & 2/3 \\ 8/3 & 10/3 \end{pmatrix}$  or  $\frac{2}{3}\sqrt{21}$  unit cell is printed in red and its mirrored domain in blue. The green circles represent a diffraction simulation performed with the *ab initio* simulated surface structure where the spot intensity corresponds to the simulated diffraction intensity. (b) Structure model of one domain with single caffeine molecules represented in red and the Au substrate in yellow. One  $\frac{2}{3}\sqrt{21}$  and a  $2\sqrt{7}$  unit cell are shown in blue and black, respectively.

molecules, the herringbone reconstruction of the substrate is still visible. The herringbone reconstruction can be used to identify a rotation angle of  $10 \pm 3^\circ$  between one hexagonal film axis and the Au $[1\bar{1}0]$  direction. Note that the STM images were taken at room temperature and distortions and slight shear are present in these measurements. To validate the values measured with STM, LEED measurements are presented later in this work. Additionally, no structural change of the herringbone reconstruction was found due to the adsorbed caffeine film, which is an indication for weak adsorbate-substrate interaction [28].

Using x-ray photoemission spectroscopy (see the Supplemental Material [15]), we found that the energy of the gold core-electron levels hardly shift upon deposition of caffeine and no new components are observed. Considering that the expected effect should be small, a more surface sensitive measurement was performed at an emission angle of  $60^\circ$  and no modification in the Au  $4f$  signal was visible. The XP spectra of C, N, and O are also very similar to the caffeine spectra in the gas phase. For more details see Sec. III B. Those two findings allow us to conclude that no noteworthy chemical interaction between molecules and substrate occurs.

Furthermore, the STM images show that the caffeine molecules are present in two distinct domains rotated by  $20 \pm 3^\circ$ , which is a consequence of the angle of  $\pm 10 \pm 3^\circ$  towards the Au $[1\bar{1}0]$  direction. Figure 3(a) shows two different domains separated by a substrate step edge, indicating the domain rotation with white and blue lines. Figure 3(b) displays the result of a fast Fourier transform (FFT) applied to the data of Fig. 3(a). It clearly reveals 12 spots corresponding to the two hexagonal domains, rotated by an angle of  $20 \pm 3^\circ$  averaged over several STM images in which both domains are present. The experimental uncertainty depends largely on the measured shear. Therefore, we consider the LEED experiment, which will be shown later in Fig. 4, to be more authoritative with respect to the measured angles.

Two types of domain borders are present in the caffeine monolayer film. One is a sharp domain border at substrate step edges, which spatially separates the domains, and is shown in Fig. 3(a). In contrast, a dividing line between both mirrored films on the same substrate terrace has been detected, as shown in Fig. 3(c) marked by a semitransparent blue line. This second boundary is a twin boundary, due to the chiral growth of the caffeine domains. These types of borders show no sharp edges, which is likely an indication of high mobility of the molecules at room temperature.

Figure 4(a) shows a LEED measurement recorded at  $E_{\text{kin}} = 20$  eV, confirming the monolayer growth in a hexagonal pattern and its two distinct domains with a rotation angle of  $11.0(8)^\circ$  towards the Au[110] direction measured across several LEED images at different energies. Note that the LEED spot intensity of the caffeine monolayer decreases for higher electron energies. Thus, the spots were not clearly visible above a kinetic energy of  $\sim 30$  eV. Therefore, it was not possible to take an image with both Au and caffeine spots at the same time, as Au(111) spots enter the screen above  $\sim 50$  eV. Instead, we used a series of images at different kinetic energies to measure the angles and distances. Excerpts of one LEED series are presented in the Supplemental Material [15]. The measured distances are plotted vs  $1/\sqrt{E}$  and fitted with a linear regression through the origin to estimate the nearest neighbor distance of caffeine in relation to a Au-Au distance of  $2.884 \text{ \AA}$  [29]. Using this method further described in [30], a nearest neighbor distance of  $8.6(3) \text{ \AA}$  was obtained from the LEED pattern, which is in perfect agreement to the nearest neighbor distance resulting from the STM measurements. The LEED image also reproduces the 2D-FFT image in Fig. 3(b), which indicates these two domains being predominantly present at the surface.

A structural analysis of the STM and LEED results, neglecting surface reconstructions, indicates a strong periodicity in form of a quasihexagonal superlattice  $\begin{pmatrix} 3.3(3) & 0.66(6) \\ 2.6(3) & 3.3(3) \end{pmatrix}$  and its mirror-symmetric counterpart  $\begin{pmatrix} 3.3(3) & 2.6(3) \\ 0.66(6) & 3.3(3) \end{pmatrix}$  with basis vectors shown in Fig. 4(b). This can be approximated as fractional numbers to be a  $\begin{pmatrix} 10/3 & 2/3 \\ 8/3 & 10/3 \end{pmatrix}$  and its corresponding mirrored  $\begin{pmatrix} 10/3 & 8/3 \\ 2/3 & 10/3 \end{pmatrix}$  unit cell. The small size of the unit cell and the possibility to formulate the epitaxy matrix in fractional numbers indicates that there is either only a single molecule per unit cell, which forms a higher-order commensurate structure, or several, chemically similar molecules in a larger, potentially commensurate unit cell. In Fig. 4(b) both unit cells are presented with a model of one domain with single caffeine adsorbates represented in red, and substrate gold atoms in yellow. The  $\begin{pmatrix} 10/3 & 2/3 \\ 8/3 & 10/3 \end{pmatrix}$  unit cell, which reads as a  $(\frac{2}{3}\sqrt{21} \times \frac{2}{3}\sqrt{21})R \pm 10.9^\circ$  unit cell in Wood notation and hereafter called  $\frac{2}{3}\sqrt{21}$  is marked in blue. The three-molecule  $\begin{pmatrix} 6 & 4 \\ 2 & 6 \end{pmatrix}$  unit cell which reads as  $(2\sqrt{7} \times 2\sqrt{7})R \pm 19.1^\circ$  unit cell in Wood notation and hereafter called  $2\sqrt{7}$  is presented in black. A short summary of the unit cell notations is given in Table I. In the figures we provide the matrix notation of the unit cells.

In order to assess the question whether all molecules are equidistantly adsorbed with the same orientation in a  $\frac{2}{3}\sqrt{21}$

TABLE I. Representation of the different unit cell notations present in this work. The epitaxy matrix notation is presented only for one domain, the mirrored domain is described by the transposed matrix. No. mols. represents the number of molecules per unit cell.

	$\frac{2}{3}\sqrt{21}$ unit cell	$2\sqrt{7}$ unit cell
Wood	$(\frac{2}{3}\sqrt{21} \times \frac{2}{3}\sqrt{21})R \pm 10.9^\circ$	$(2\sqrt{7} \times 2\sqrt{7})R \pm 19.1^\circ$
Matrix	$\begin{pmatrix} 10/3 & 2/3 \\ 8/3 & 10/3 \end{pmatrix}$	$\begin{pmatrix} 6 & 4 \\ 2 & 6 \end{pmatrix}$
No. mols.	1	3

unit cell or whether they are adsorbed with varying positions and rotations in a three times larger commensurate  $2\sqrt{7}$  unit cell, we generated the respective LEED pattern using the package LEEDpat [31] and depicted them in Fig. 4(a). The LEED pattern arising from the  $\frac{2}{3}\sqrt{21}$  unit cell is shown in the right half of the LEED image, while the left half displays the result for the commensurate  $2\sqrt{7}$  unit cell. Red and blue circles represent the spots for each domain subpattern. Note that the generated LEED patterns at this stage only account for the periodicity of the unit cell and not for the intensity of the spots, which originates from the electronic structure (i.e., the structure factor) of the contents of the unit cell.

At this point, we employ *ab initio* simulations to gain further insight into the monolayer formation. Taking into account the weak interaction between molecules and substrate we can model the surface system from first principles with density functional theory in a three-step procedure. In a first step we map the chemical interactions between pairs of molecules in a free-standing monolayer of caffeine molecules to gain insight into the molecule-molecule interactions. Then, as a second step, we simulate the full molecule-substrate system to show that the adsorption on Au(111) does not lead to substantial changes in the physics of the system. As a third step we simulate the diffraction pattern of the full molecular monolayer using kinematic diffraction theory. The simulated diffraction intensities are plotted as green circles in the lower half of Fig. 4(a).

For the first step we modeled all possible interactions between two molecules in a hypothetical free-standing monolayer. To do so, we first optimized the geometry of an isolated caffeine molecule and then oriented the quasiplanar molecule parallel to the surface orientation ( $xy$  plane). Second, we calculated the interaction energy between one fixed molecule and a second one at different locations and rotations relative to the first molecule. Because we cannot calculate all continuous relative arrangements exhaustively, we introduced a suitable discretization: For the translational discretization we used a hexagonal grid with a spacing of  $0.738 \text{ \AA}$  (1/4th of the minimal Au-Au distance of the simulation). The molecule was allowed to rotate in steps of  $30^\circ$  around the central pyrimidine ring. The fact that caffeine can adsorb on the surface in two mirror-symmetric ways leads to two fundamentally different cases on the surface, namely the interaction of two molecules with same, and two molecules with different on-surface chirality.

Figure 5 shows the interaction energies between two caffeine molecules without substrate. An attractive and repulsive interaction of the respective molecule pair is represented by

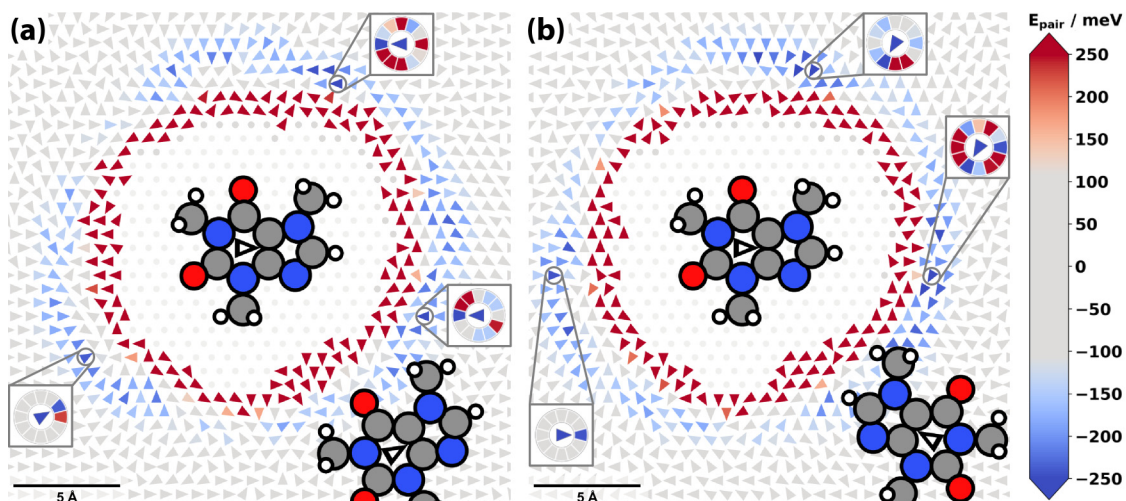


FIG. 5. Discretized pairwise interactions of caffeine molecules in a free-standing monolayer in two chiral arrangements (a) and (b). In the bottom right corner of both plots the in-plane geometry of a molecule, relative to the centered fixed molecule, is shown with the corresponding arrow in the center of the pyrimidine ring. The arrows represent the energetically most favorable in-plane rotation of the second caffeine molecule at each respective location. The insets visualize the interaction energies for all different rotations at the energetically most favorable positions in each of the three energetically favorable areas. (a) Pair interaction energies for both molecules with the same on-surface chirality. (b) Pair interaction energy results for different surface chirality.

blue and red colors, respectively. The arrows indicate the energetically most favorable orientation of the second molecule with respect to the fixed central one for each discretized position. In the bottom right corner of both plots, the in-plane geometry of a molecule, relative to the centered fixed molecule, is shown with its corresponding arrow in the center of the pyrimidine ring.

When both molecules have the same on-surface chirality, as shown in Fig. 5(a), there are three distinct regions where the interaction is attractive. Importantly, in neither of these regions is it energetically favorable to align the molecule parallel; rather, it is energetically more favorable to align them antiparallel or slightly rotated with respect to each other. Similarly, when both molecules exhibit the opposite on-surface chirality, the energetically most favorable interaction is obtained when rotating the molecules relative to each other as shown in Fig. 5(b). An exception to this rule is the region on the left side of Fig. 5(b) where a parallel alignment of mirrored molecules is favorable. This could only explain 1D lines, consisting of at least two prochiral molecules per unit cell, and cannot be used to build full 2D homochiral surface structures. As a consequence, it seems unlikely that caffeine would form a monolayer with a single molecule per unit cell, where all molecules would have to be oriented the same way.

With these findings we can dismiss the possibility of a unit cell containing only a single molecule, as this would require a parallel alignment, which is energetically highly unfavorable. Instead, the true surface structure model must contain more than one molecule in the unit cell. For this surface structure model, we consider the monolayer film as the smallest superlattice, which is commensurate with the Au(111) substrate. This superlattice is described by the  $2\sqrt{7}$  unit cell which retains hexagonal symmetry, has a lattice constant of 15.2 Å with respect to an unreconstructed Au(111) surface, and contains three molecules. It is shown in black in

Fig. 4(b). For this unit cell, neglecting the structure factors, the LEEDpat simulation is plotted in red and its mirrored counterpart in blue circles at the top of the left side of Fig. 4(a). Based on the LEEDpat simulation one would expect that the larger  $2\sqrt{7}$  unit cell yields more LEED spots, which is indicated in Fig. 4(a) on the left side.

To get more insight into the geometric arrangement of the tight-packed molecular monolayer, we tried to find the energetically most favorable caffeine arrangement within this given supercell. For this purpose, we used parts of the ideas of the structure-search algorithm SAMPLE [32], as explained hereafter. Within the above-described discretization, we first set up all possible structures with three caffeine molecules that fit into the unit cell. Then we used the interaction energies calculated in the gas-phase to evaluate the relative energies of all those possible structures. A ranking of all possibilities reveals the energetically most favorable structure, which manages best to counterbalance repulsion caused by tight packing and attraction due to favorable intermolecular interactions. Note that due to the tight-packing constraint the energetically most favorable pairs are not necessarily part of the best densely packed structure. A geometry optimization of the best structure on the Au(111) surface yields an adsorption energy of around  $-1.1$  eV per caffeine molecule, which is in the expected energy range for physisorption of molecules of this size [33,34]. Notably, the found structure requires a heterochiral assembly of caffeine molecules to get an energetically favorable structure. In this assembly the ratio of caffeine molecules of both on-surface chiralities is 1 : 2 and vice versa for the mirrored domain. During the optimization the caffeine geometry did not change substantially, which corroborates the applicability of the two-step approach. The optimized structure is shown in Fig. 6 and was then used to calculate the core level shifts. For further details, the whole simulation results are available free of charge through the NOMAD database under [35].

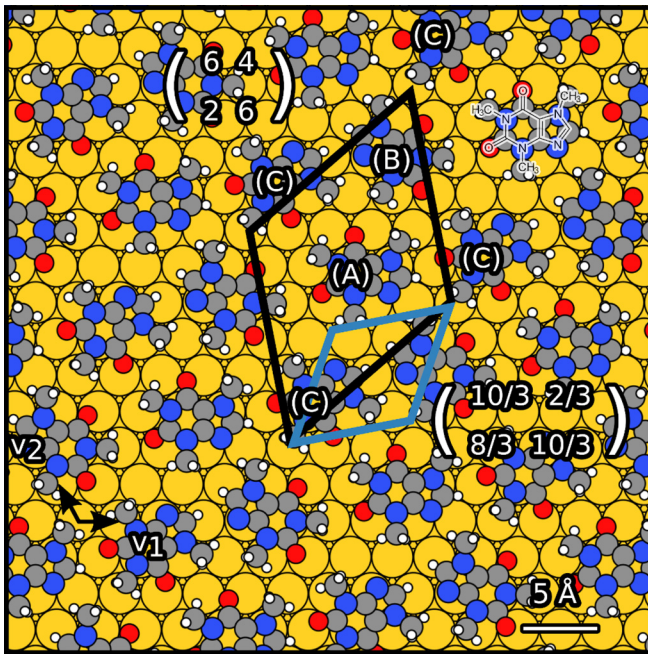


FIG. 6. Geometry-optimized monolayer of caffeine with three molecules in a  $\begin{pmatrix} 6 & 4 \\ 2 & 6 \end{pmatrix}$  or  $2\sqrt{7}$  unit cell on Au(111). The three molecules within a unit cell are aligned in the structure that yields the best energy per area (rather than per molecule), balancing out repulsive interactions due to tight packing with attractive intermolecular interactions. The three molecular orientations are marked by letters A, B, and C. The surface basis vectors  $v_1$  and  $v_2$  are indicated. The radii used for the atoms shown are 1.2 times the respective covalent radii.

At this point, one question remains unanswered: If the unit cell is three times the size, why does the LEED pattern fail to exhibit the additional spots indicated in Fig. 4(a)? To answer this question, we performed a diffraction simulation using the atomistic geometry of our calculated structure (as visualized in Fig. 6) and kinematic scattering theory. This simulation takes local atomic structure factors, and thus extinction of superfluous peaks, into account. The results are depicted in Fig. 4(a) with green circles, where the intensity of the peaks represents the calculated diffraction intensities. The diffraction simulation shows that the first-order spots for the three-molecule structure in a  $2\sqrt{7}$  unit cell are very weak with an intensity ratio of approximately 1 : 33 compared to the bright spots corresponding to the first order of a  $\frac{2}{3}\sqrt{21}$  unit cell. Thus, the diffraction simulation provides a suitable explanation for the lack of an observable signal of the three-molecule unit cell, as the seemingly superfluous peaks almost vanish due to in-cell extinction.

The hypothesis with three molecules per unit cell is also in accordance with previous studies of caffeine in the high-temperature  $\alpha$ -phase polymorph [2,4]. Derollez *et al.* proposed a structure for  $\alpha$ -caffeine in a trigonal bulk crystal including a dynamically disordered relation of the caffeine molecules in a  $R3c$  space-group unit cell. The estimated parameters of the trigonal unit cell are  $a = 14.94 \text{ \AA}$  and  $c = 6.90 \text{ \AA}$  [2]. Their proposed lattice constant is in excellent accordance with our estimated value of  $15.2 \text{ \AA}$ . In the unit

cell they assumed two quasi-hexagonal layers of caffeine molecules with a height difference of  $\pm c/6$  for alternating molecules in one layer. For a monolayer, this height difference is not expected and we could not find any indications for it in our measurements. The previously estimated molecule nearest neighbor distance of  $8.6(3) \text{ \AA}$ , as suggested by the STM and LEED data, is in accordance with the three-molecule unit cell model, since there is a uniform distribution of molecules within the unit cell.

### B. Core level photoemission spectroscopy

XPS measurements were carried out in order to study the surface and intermolecular interactions. To test our hypothesis, we compare the experimental data of the C 1s, N 1s, and O 1s electrons of the monolayer film with the core levels of the hypothetical, free-standing adsorbate (shown in Fig. 6) obtained by DFT. The preparation of the caffeine monolayer was performed as described in the method section and was validated by LEED. All XP spectra were fitted by applying a convolution of a Doniach-Sunjić, a Gauss function, and a Tougaard background. The molecules' XP spectra are compared with the molecular core levels in the initial-state approximation, which assumes the relative core-level eigenvalue shifts of the undisturbed system to correspond to relative XPS peak shifts. We expect that surface effects affect all atoms the same way. The calculated results were aligned against the experimental peak with highest kinetic energy for an easy comparison of relative shifts of single components [36].

The molecular core levels were broadened by a Voigt profile with respective Gauss and Lorentz parameters in accordance with experiment. To reduce complexity and increase interpretability, the molecular core levels of the three molecules were grouped into chemically related components, which are indicated in the spectra. All components' grouped simulated energy positions are presented in the Supplemental Material [15].

Figure 7 shows the C 1s signal, recorded with a photon energy of  $h\nu = 340 \text{ eV}$  and at normal emission. It consists of five different components, resulting from a sum of the signals of eight carbon atoms within the caffeine molecule. Component A was found at a kinetic energy of  $E_{\text{kin}} = 51.94 \text{ eV}$  with  $\Delta E = 1.1 \text{ eV}$  full width at half maximum (FWHM), an asymmetry factor of  $\alpha = 0.05$ , and an area of 49% of the complete signal. With the results of Plekan *et al.* [14] on gas-phase caffeine, component A is assigned to the carbon atoms C5, C10, C12, and C14 as labeled in Fig. 1. Component B is assigned to C8 and C4. C is assigned to the carbon atom C6. Component D is assigned to the carbon atom C2. A satellite peak caused by a  $\pi \rightarrow \pi^*$  transition was found in the signal with an energy of  $-4.51 \text{ eV}$  relative to A with FWHM of  $1.7 \text{ eV}$ ,  $\alpha = 0.07$ , and an amount of 7% of the complete signal, which is common in organic adsorbate XPS [37].

For the C 1s signal all experimentally estimated values and the relative energy shifts for the experiment and simulation are shown in Table II. Figure 7 compares the experimental spectrum with the shifts obtained by the DFT calculations, showing a well reproduced line shape. The respective kinetic energies of the components of the simulated spectrum are shown in the Supplemental Material [15]. The relative energy

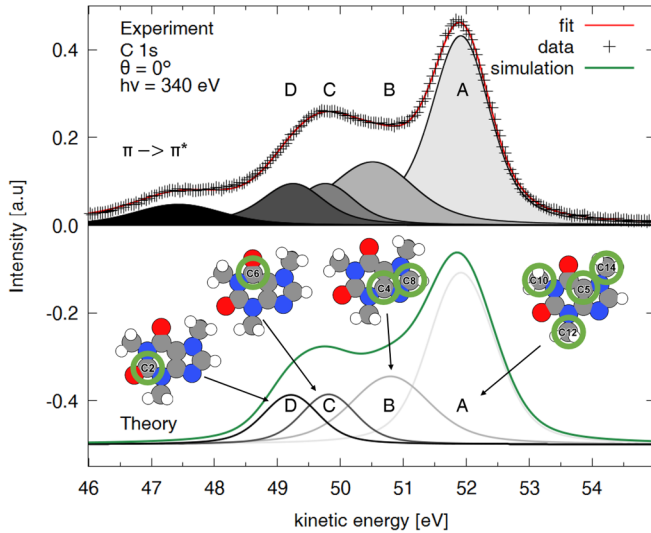


FIG. 7. C  $1s$  core-level XPS of caffeine on Au(111) recorded at a photon energy of  $h\nu = 340$  eV and at an emission angle of  $\Theta = 0^\circ$ . The assignment of carbon atoms A, B, C, and D is indicated by green circles. In the bottom panel, the simulated XP spectrum of the caffeine monolayer is shown.

shift  $\Delta E_{\text{sim}}$  in Table II refers to component A of the carbon  $1s$  signal. The computed difference between the peaks of components A and B is 0.25 eV lower than in the experiment. The computed energy differences of components C and D with respect to A agree within 0.1 eV with the experimental analysis.

Figure 8 displays the N  $1s$  signal recorded at a photon energy of  $h\nu = 500$  eV. The spectrum consists of four components, corresponding to the four nitrogen atoms of the molecule. Each component amounts to  $\sim 25\%$  of the signal area, with a FWHM of  $\sim 1.4$  eV, and an asymmetry factor of  $\alpha \sim 0.02$ . All experimentally estimated values and the relative energy shifts for the experiment and simulation of the N  $1s$  signal are shown in Table III. The energy difference between the simulated components N1, N3, and N7 is smaller than the measured experimental difference between those components. The signals of N1 and N7 are separated by 1.05 and 0.60 eV in the experimental and simulated data, respectively. In comparison to gas-phase caffeine, the FWHM values are increased as expected [38]. The comparison of the experimental data to the

TABLE II. Experimental and simulated C  $1s$  core-level XPS energy shifts for caffeine on Au(111) assigned to the different components which are shown in Fig. 7. In addition, the experimental full width at half maximum (FWHM), asymmetry factors  $\alpha$ , and the relative area of the components are shown.

C $1s$	$E_{\text{kin}}$ (eV)	$\Delta E_{\text{sim}}$ (eV)	FWHM (eV)	$\alpha$	Rel. area
A	51.94		1.1	0.05	49%
B	-1.39	-1.14	1.6	0.05	23%
C	-2.15	-2.12	1.1	0.05	10%
D	-2.66	-2.72	1.2	0.05	11%
$\pi \rightarrow \pi^*$	-4.51		1.7	0.07	7%

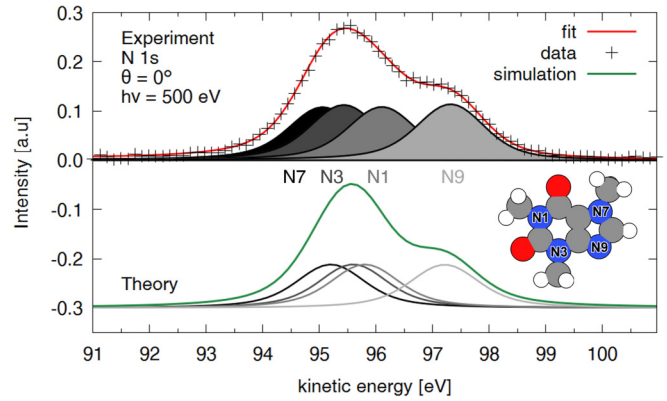


FIG. 8. N  $1s$  core-level XPS of caffeine on Au(111) recorded at a photon energy of  $h\nu = 500$  eV and at an emission angle of  $\Theta = 0^\circ$ . The simulated XP spectrum of the caffeine monolayer is shown in the bottom panel.

DFT simulation on Au(111) shows a good agreement between the two spectra.

Additionally, the oxygen O  $1s$  signal was recorded at a photon energy of  $h\nu = 650$  eV, as shown in Fig. 9. The individual signals of the two oxygen atoms were not separated in the spectrum, thus only one component was observed. This component is located at a kinetic energy of  $E_{\text{kin}} = 114.44$  eV with  $\Delta E = 1.8$  eV FWHM, and an asymmetry factor of  $\alpha = 0.08$ . Also, the energy difference between the two components calculated in the simulation is small with  $\Delta E = 0.08$  eV and could not be resolved in the experiment. We thus would not expect it to be resolvable experimentally.

The XP spectra of adsorbed caffeine are in excellent accordance with previous XPS results of caffeine molecules in gas phase by Plekan *et al.* [14], and with our calculated values. In our experimental XPS analysis we cannot distinguish between different molecular unit cells, and we cannot disprove the three-molecular unit cell. Since a single molecular unit cell is proven unlikely by the other methodologies, we consider that all performed measurements support the three-molecular unit cell hypothesis.

#### IV. CONCLUSION

In this work we found the formation of a densely packed monolayer of caffeine molecules on Au(111) in two different domains. The molecules form a quasihexagonal structure with

TABLE III. Experimental and simulated N  $1s$  core-level XPS energy shifts for caffeine on Au(111) assigned to the different components which are shown in Fig. 8. In addition, the experimental full width at half maximum (FWHM), asymmetry factors  $\alpha$  and the relative area of the components are shown.

N $1s$	$E_{\text{kin}}/\Delta E$ (eV)	$\Delta E_{\text{sim}}$ (eV)	FWHM (eV)	$\alpha$	Rel. area
N9	97.33		1.4	0.02	26%
N1	-1.21	-1.41	1.4	0.02	25%
N3	-1.89	-1.62	1.4	0.02	25%
N7	-2.26	-2.01	1.4	0.02	24%

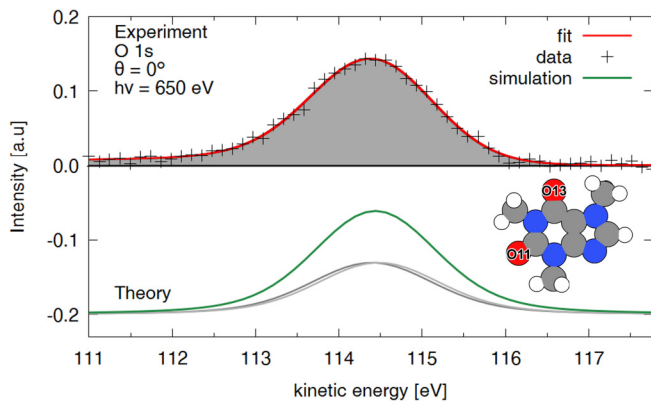


FIG. 9. O 1s core-level XPS of caffeine on Au(111) recorded at a photon energy of  $h\nu = 650$  eV and at an emission angle of  $\Theta = 0^\circ$ . The bottom panel shows the simulated XP spectrum of the caffeine monolayer.

a nearest neighbor distance of  $8.6(3)$  Å and an angle of  $\pm 11.0(8)^\circ$  towards the  $[1\bar{1}0]$ -Au axis for each domain, respectively. This quasi-hexagonal structure was observed in real space with STM and in reciprocal space with LEED and can be described as a  $\begin{pmatrix} 10/3 & 2/3 \\ 8/3 & 10/3 \end{pmatrix}$  and its corresponding mirrored  $\begin{pmatrix} 10/3 & 8/3 \\ 2/3 & 10/3 \end{pmatrix}$  unit cell or as  $(\frac{2}{3}\sqrt{21} \times \frac{2}{3}\sqrt{21})R \pm 10.9^\circ$  with respect to an unreconstructed Au(111) surface. The further investigation with DFT calculations of a hypothetical free-standing monolayer dismissed this hexagonal superstructure with only one molecule in the unit cell. This is due to the fact that the energetically most favorable in-plane rotations between two molecules are different for the different positions. Therefore, a configuration of differently oriented molecules is energetically favorable compared to a structure with all molecules aligned in the same orientation. Taking this into account, we can describe the caffeine monolayer with a  $\begin{pmatrix} 6 & 4 \\ 2/3 & 6 \end{pmatrix}$  and its mirrored  $\begin{pmatrix} 6 & 2 \\ 4 & 6 \end{pmatrix}$  superlattice or  $(2\sqrt{7} \times 2\sqrt{7})R \pm 19.1^\circ$  with three caffeine molecules within a unit cell and a lattice constant of  $15.2$  Å. This superstructure is the smallest commensurable surface structure on the Au(111) surface, which is in accordance with the experimental results. With

this superlattice we conducted *ab initio* simulations of the intermolecular interactions in combination with monolayer structure search, which led to a proposed geometrical structure, as shown in Fig. 6. This structure is in accordance with the found LEED pattern as the diffraction simulation shows that the intensity of the additional spots of the three-times larger unit cell is 33 times weaker which was not resolvable in our experiment. The simulation suggests physisorption with low substrate-energy corrugation. Furthermore, the optimized structure predicts a mixture of both on-surface chiralities of caffeine in the unit cell for an energetically favorable alignment. The ratio of both chiralities is 1 : 2 and vice versa for the mirrored domain. In addition, the shifts of the calculated molecular orbital energies are in accordance to the experimental XPS results.

The caffeine monolayer structure found here is in excellent accordance with previous studies on different substrates. A hexagonal crystal structure was also found in surface mediated crystals on substrates like silicon, silver, soda lime glass, and silver subsurface ion-exchanged soda-lime silicate (SIMO) glasses [5]. Similar results were found for the layers of metastable hexagonal bulk crystals of caffeine discovered by Derollez *et al.* [2].

Our structural model also highlights the influence of the prochiral character of the achiral caffeine molecule on the monolayer growth on Au(111). Therefore, the prochiral character might play a role in the formation of surface mediated crystals on other substrates like the ionic crystals studied by Röthel *et al.* [7].

## ACKNOWLEDGMENTS

The authors are grateful for financial support by German federal state North Rhine-Westphalia the Land Nordrhein-Westfalen and by the Austrian Science Fund (FWF): P28631-N36 and Y1157. The computational results presented have been achieved using the Vienna Scientific Cluster (VSC). The authors thank the DELTA staff for their support during and outside beamtimes and J. Westphal for his helpful suggestions to the manuscript.

- [1] A. Nehlig, J.-L. Daval, and G. Debry, Caffeine and the central nervous system: Mechanisms of action, biochemical, metabolic and psychostimulant effects, *Brain Res. Rev.* **17**, 139 (1992).
- [2] P. Derollez, N. T. Correia, F. Danède, F. Capet, F. Affouard, J. Lefebvre, and M. Descamps, Ab initio structure determination of the high-temperature phase of anhydrous caffeine by X-ray powder diffraction, *Acta Crystallogr. Sect. B* **61**, 329 (2005).
- [3] C. W. Lehmann and F. Stowasser, The crystal structure of anhydrous beta-caffeine as determined from X-ray powder-diffraction data, *Chem.: Eur. J.* **13**, 2908 (2007).
- [4] J. Leiterer, F. Emmerling, U. Panne, W. Christen, and K. Rademann, Tracing coffee tabletop traces, *Langmuir* **24**, 7970 (2008).
- [5] A. Sarfraz, A. Simo, R. Fenger, W. Christen, K. Rademann,

- U. Panne, and F. Emmerling, Morphological diversity of caffeine on surfaces: Needles and hexagons, *Cryst. Growth Des.* **12**, 583 (2012).
- [6] C. Röthel, M. Radziown, R. Resel, A. Zimmer, C. Simbrunner, and O. Werzer, Complex behavior of caffeine crystallites on muscovite mica surfaces, *Cryst. Growth Des.* **15**, 4563 (2015).
- [7] C. Röthel, M. Radziown, R. Resel, A. Grois, C. Simbrunner, and O. Werzer, Crystal alignment of caffeine deposited onto single crystal surfaces via hot-wall epitaxy, *Cryst. Eng. Commun.* **19**, 2936 (2017).
- [8] O. Stetsovych, M. Švec, J. Vacek, J. V. Chocholoušová, A. Jančařík, J. Rybáček, K. Kosmider, I. G. Stará, P. Jelínek, and I. Starý, From helical to planar chirality by on-surface chemistry, *Nat. Chem.* **9**, 213 (2017).

- [9] F. Zaera, Chirality in adsorption on solid surfaces, *Chem. Soc. Rev.* **46**, 7374 (2017).
- [10] M. Pividori, C. Dri, M. E. Orselli, F. Berti, M. Peressi, and G. Comelli, Spontaneous symmetry breaking on ordered, racemic monolayers of achiral theophylline: Formation of unichiral stripes on Au(111), *Nanoscale* **8**, 19302 (2016).
- [11] C. Seidel, Charakterisierung organischer Adsorbate auf Silbereinkristallen mit den Meßmethoden LEED und STM, Ph.D. thesis, Universität Stuttgart, Stuttgart, 1993.
- [12] M. U. Zubair, M. M. Hassan, and I. A. Al-Meshal, Caffeine, in *Analytical Profiles of Drug Substances and Excipients*, Analytical Profiles of Drug Substances, Vol. 15, edited by K. Florey and H. G. Brittain (Academic, New York, 1972-2002), pp. 71–150.
- [13] NIST Mass Spectrometry Data Center, W. E. Wallace, director, Mass Spectra, in *NIST Chemistry WebBook, NIST Standard Reference Database Number 69*, edited by P.J. Linstrom and W.G. Mallard (NIST, Gaithersburg, MD, 2018) p. 20899.
- [14] O. Plekan, V. Feyer, R. Richter, A. Moise, M. Coreno, K. C. Prince, I. L. Zaytseva, T. E. Moskovskaya, D. Y. Soshnikov, and A. B. Trofimov, X-ray spectroscopy of heterocyclic biochemicals: Xanthine, hypoxanthine, and caffeine, *J. Phys. Chem. A* **116**, 5653 (2012).
- [15] See Supplemental Material at <http://link.aps.org/supplemental/10.1103/PhysRevB.101.245414> for XP spectra of the Au 4f signal showing no chemical interactions between the caffeine molecules and the Au substrate. Also, tables with the calculated core levels of the adsorbate are presented there (Refs. [39–42]).
- [16] D. Nečas and P. Klapetek, Gwyddion: An open-source software for SPM data analysis, *Open Phys.* **10**, 99 (2012).
- [17] C. Westphal, U. Berges, S. Dreiner, R. Follath, M. Krause, F. Schäfers, D. Schirmer, and M. Schürmann, The plane-grating monochromator beamline at the U55 undulator for surface and interface studies at DELTA, *J. Electron Spectrosc. Relat. Phenom.* **144-147**, 1117 (2005).
- [18] S. Doniach and M. Sunjic, Many-electron singularity in x-ray photoemission and x-ray line spectra from metals, *J. Phys. C: Solid State Phys.* **3**, 285 (1970).
- [19] S. Tougaard, Quantitative analysis of the inelastic background in surface electron spectroscopy, *Surf. Interface Anal.* **11**, 453 (1988).
- [20] N. Mårtensson and A. Nilsson, Core-level line shapes of adsorbates: Effects of electronic and vibrational excitations, *J. Electron Spectrosc. Relat. Phenom.* **52**, 1 (1990).
- [21] R. Hesse and R. Denecke, Improved Tougaard background calculation by introduction of fittable parameters for the inelastic electron scattering cross-section in the peak fit of photoelectron spectra with UNIFIT 2011, *Surf. Interface Anal.* **43**, 1514 (2011).
- [22] V. Blum, R. Gehrke, F. Hanke, P. Havu, V. Havu, X. Ren, K. Reuter, and M. Scheffler, Ab initio molecular simulations with numeric atom-centered orbitals, *Comput. Phys. Commun.* **180**, 2175 (2009).
- [23] J. P. Perdew, K. Burke, and M. Ernzerhof, Generalized Gradient Approximation Made Simple, *Phys. Rev. Lett.* **77**, 3865 (1996).
- [24] V. G. Ruiz, W. Liu, E. Zojer, M. Scheffler, and A. Tkatchenko, Density-Functional Theory with Screened van der Waals Interactions for the Modeling of Hybrid Inorganic-Organic Systems, *Phys. Rev. Lett.* **108**, 146103 (2012).
- [25] H. J. Monkhorst and J. D. Pack, Special points for Brillouin-zone integrations, *Phys. Rev. B* **13**, 5188 (1976).
- [26] J. Neugebauer and M. Scheffler, Adsorbate-substrate and adsorbate-adsorbate interactions of Na and K adlayers on Al(111), *Phys. Rev. B* **46**, 16067 (1992).
- [27] C. Colliex, J. Cowley, S. Dudarev, M. Fink, J. Gjønnnes, R. Hilderbrandt, A. Howie, D. Lynch, L. Peng, G. Ren *et al.*, Electron diffraction, *Internatl. Tables Crystallogr. C*, 259 (2006).
- [28] F. Hanke and J. Björk, Structure and local reactivity of the Au(111) surface reconstruction, *Phys. Rev. B* **87**, 235422 (2013).
- [29] A. Maeland and T. B. Flanagan, Lattice spacings of gold-palladium alloys, *Can. J. Phys.* **42**, 2364 (1964).
- [30] M. Lackinger, S. Griessl, W. M. Heckl, and M. Hietschold, Coronene on Ag (111) investigated by LEED and STM in UHV, *J. Phys. Chem. B* **106**, 4482 (2002).
- [31] LEEDpat, Version 4.2, utility by K.E. Hermann (FHI) and M.A. Van Hove (HKBU), Berlin / Hong Kong, 2014; see also <http://www.fhi-berlin.mpg.de/KHsoftware/LEEDpat/index.html>.
- [32] L. Hörmann, A. Jeindl, A. T. Egger, M. Scherbela, and O. T. Hofmann, SAMPLE: Surface structure search enabled by coarse graining and statistical learning, *Comput. Phys. Commun.* **244**, 143 (2019).
- [33] P. Sony, P. Puschnig, D. Nabok, and C. Ambrosch-Draxl, Importance of van der Waals Interaction for Organic Molecule-Metal Junctions: Adsorption of Thiophene on Cu(110) As a Prototype, *Phys. Rev. Lett.* **99**, 176401 (2007).
- [34] L. Romaner, D. Nabok, P. Puschnig, E. Zojer, and C. Ambrosch-Draxl, Theoretical study of PTCDA adsorbed on the coinage metal surfaces, Ag(111), Au(111) and Cu(111), *New J. Phys.* **11**, 053010 (2009).
- [35] A. Jeindl, Simulation Data of Caffeine on Au(111), *NOMAD* (2020).
- [36] M. Giesbers, A. T. M. Marcelis, and H. Zuilhof, Simulation of XPS C1s spectra of organic monolayers by quantum chemical methods, *Langmuir* **29**, 4782 (2013).
- [37] A. Schöll, Y. Zou, M. Jung, T. Schmidt, R. Fink, and E. Umbach, Line shapes and satellites in high-resolution x-ray photoelectron spectra of large pi-conjugated organic molecules, *J. Chem. Phys.* **121**, 10260 (2004).
- [38] M. Wiklund, A. Jawarowski, F. Strisland, A. Beutler, A. Sandell, R. Nyholm, S. L. Sorensen, and J. N. Andersen, Vibrational fine structure in the C 1s photoemission spectrum of the methoxy species chemisorbed on Cu(100), *Surf. Sci.* **418**, 210 (1998).
- [39] K. Asami, A precisely consistent energy calibration method for X-ray photoelectron spectroscopy, *J. Electron Spectrosc. Relat. Phenom.* **9**, 469 (1976).
- [40] K. Heister, M. Zharnikov, M. Grunze, and L. S. O. Johansson, Adsorption of Alkanethiols and Biphenylthiols on Au and Ag Substrates. A High-Resolution X-ray Photoelectron Spectroscopy, *Study. J. Phys. Chem. B* **105**, 4058 (2001).
- [41] P. Heimann, J. F. van der Veen, and D. E. Eastman, Structure-dependent surface core level shifts for the Au(111), (100), and (110) surfaces, *Solid State Commun.* **38**, 595 (1981).
- [42] G. K. Wertheim and S. B. Diczienzo, Least-squares analysis of photoemission data, *J. Electron Spectrosc. Relat. Phenom.* **37**, 57 (1985).